research articles Journal of proteome research

Kinetic Binding Analysis of Aptamers Targeting HIV-1 Proteins by a Combination of a Microbalance Array and Mass Spectrometry (MAMS)

Thomas M. A. Gronewold,[†] Antje Baumgartner,[†] Jessica Hierer,[†] Saleta Sierra,[‡] Michael Blind,[§] Frank Schäfer,[||] Julia Blümer,[||] Tina Tillmann,[||] Anne Kiwitz,[†] Rolf Kaiser,[‡] Martin Zabe-Kühn,[†] Eckhard Quandt,*[,†,⊥] and Michael Famulok*[,†,#]

Research Center CAESAR, Ludwig-Erhard-Allee 2, D-53175 Bonn, Germany, Institute of Virology of the University Cologne, Fürst Pückler Strasse 56, D-50935 Cologne, Germany, Menterstrasse 141, D-81247 München, Germany, QIAGEN GmbH, Qiagen Str. 1, D-40724 Hilden, Germany, Faculty of Engineering, University of Kiel, Kaiserstrasse 2, D-24143 Kiel, Germany, and LIMES Institute, Program Unit Chemical Biology & Medicinal Chemistry, University of Bonn, Gerhard-Domagk-Strasse 1, D-53121 Bonn, Germany

Received March 20, 2009

An enhanced chip-based detection platform was developed by integrating a surface acoustic wave biosensor of the Love-wave type with protein identification by matrix-assisted laser desorption/ionization time-of-flight mass spectrometry (MALDI-ToF MS). The system was applied to characterize the interaction of aptamers with their cognate HIV-1 proteins. The aptamers, which target two proteins of HIV-1, were identified using an automated *in vitro* selection platform. For aptamers S66A-C6 and S68B-C5, which target the V3 loop of the HIV-1 envelope protein gp120, K_D values of 406 and 791 nM, respectively, were measured. Aptamer S69A-C15 was shown to bind HIV-1 reverse transcriptase (HIV-1 RT) with a K_D value of 637 nM when immobilized on the biosensor surface. HIV-1 RT was identified with high significance using MALDI-ToF MS even in crude protein mixtures. The V3-loop of gp120 could be directly identified when using chip-bound purified protein samples. From crude protein mixtures, it could be identified indirectly with high significance via its fusion-partner glutathione-*S*-transferase (GST). Our data show that the combination of the selectivity of aptamers with a sensitive detection by MS enables the reliable and quantitative analysis of kinetic binding events of protein solutions in real time.

Keywords: Love-Wave Surface Acoustic Wave Sensor • Affinity-MS • MALDI-ToF MS • HIV gp120 • HIV Reverse Transcriptase

Introduction

The combination of quantification and purification of proteins by various chip-based biosensors with identification by mass spectrometry (MS) has been reported more than a decade ago.[1,2] Since then, affinity-MS has become a powerful tool in proteomics. It enables the detection and analysis even of small amounts of known and unknown proteins interacting in complex biological networks, yielding information on the interaction process and the molecular masses of the analytes. MS allows identification of proteins and differentiation of post-translational modifications within otherwise identical proteins, for example, glycosylations or phosphorylations. To date, MS is one of the most sensitive and specific methods for protein identification. A disadvantage of MS, however, is the difficult quantification.[3] To address this issue, we have combined MS with preceding monitoring of binding using a biosensor[4] that enables label-free quantification of the mass of an analyte protein[5] or the determination of its amount.[6] Specific interactions take place between the mobile analytes in solution and the immobilized ligands, resulting in selective binding events displayed in the recorded sensor signal. The ligands immobilized on the chip surface specify the detected analytes and allow the characterization of the biomolecular interactions.[7] Such binding of a given, predefined subset of molecules from an unpurified sample or mixture can be put to use for tracked precleaning of analytes in a way that keeps the bound molecules undestroyed. Applied to proteins, the surface may bind a specific protein, its variants, or complexes thereof, depending on both the affinity and quality of the ligand, but also on the surface chemistry used for immobilization. Thus, for identification of the surface-bound proteins, they can further be analyzed by MS.[8] To sense mass changes from binding events, different

* To whom correspondence should be addressed. E-mail: (E.Q.) eq@tf.uni-kiel.de, (M.F.) m.famulok@uni-bonn.de.
[†] Research Center CAESAR.
[‡] Institute of Virology of the University Cologne.
[§] Menterstrasse 141.
[||] QIAGEN GmbH.
[⊥] University of Kiel.
[#] University of Bonn.

10.1021/pr900265r CCC: $40.75
Published on Web 05/27/2009

types of sensors are used. Commercial examples are sensors based on the surface plasmon resonance (SPR) principle. The very small volumes of the surface-bound proteins are eluted after capture to be measured in MALDI-ToF MS.[9] This combination, however, is labor-intensive and usually not compatible with high-throughput analyses.

Here, we combined a surface acoustic wave sensor of the Love-wave type (the S-sens K5-sensor system) with MALDI-ToF MS measurements.[5,6] This system is based on a noninvasive technique that detects phase and amplitude changes in real time. In parallel, mass and viscosity alterations are analyzed, providing additional information about the observed binding event. Extremely low response to buffer contents enables the interpretation of data directly from the recorded signal. Furthermore, the technique is not limited to gold-based surface chemistries, thus, allowing the use of customized sensor chip surfaces based on metals, oxides, or polymers. Here, in a pilot setting, we applied the method to characterize a set of aptamers targeted against HIV-1 proteins.

Aptamers are synthetic nucleic acid ligands, which are able to bind to target proteins with high specificities and affinities.[10−17] They have successfully been used as capture agents in previous sensor chip applications, for example, as receptors to capture thrombin molecules from complex mixtures on glass surfaces. The thrombin was released from the aptamer surface by a pH-shift for further analysis in the MALDI-ToF-MS.[18] The combination of aptamers with various biosensors has proven suitable for monitoring the analyte even in complex protein mixtures.[19−22] Both thrombin and antithrombin III and an immobilized thrombin−antithrombin III protein complex were detected on the chip with MALDI-ToF-MS.[8] Several standardized *in vitro* selection protocols for advanced production of aptamers have been established modifying the original SELEX (systematic evolution of ligands by exponential enrichment) procedure[23,24] for automated high-throughput selections.[25,26]

Here, we used an automated procedure based on biotinylated proteins binding to magnetic beads on a robotics workstation to parallelize the selection of aptamers. Proteins were expressed as fusion proteins with glutathione *S*-transferase (GST-V3).[27] The first two targets for proof-of-principle studies were the third variable loop of gp120 (V3) and reverse transcriptase (RT), both proteins of human immunodeficiency virus type 1 (HIV-1). V3 is highly immunogenic, but linear epitopes of V3 are highly variable in sequence.[28,29] Anti-gp120 aptamers have been shown to neutralize R5 strains of HIV-1.[30] HIV-1 RT is a DNA polymerase enzyme that uses RNA or DNA strands as templates. It transcribes single-stranded viral RNA into double-stranded DNA during the replicative cycle. Several anti-HIV-1 RT aptamers have been described[31−34] and were shown to inhibit HIV-1 replication.[31,35−37] Recently, an anti-HIV-1 RT aptamer-dependent ribozyme[38] was used in a screening assay to identify a small molecule inhibitor that showed a similar inhibitory profile as the parent aptamer.[39] The target in this study was a RT variant RT948-2 isolated from a patient sample by the Virology group at the University of Cologne. It is highly homologous to the previously described HIV-1 RT samples[40,41] AAO63179 and AAD03191.

Experimental Section

All chemicals were of analytical grade, unless otherwise noted, and were used without further purification. 11-Mercapto-1-undecanol (44,752-8), *N*-hydroxysuccinimide (NHS, H-7377), dextran from *Leuconostoc mesenteroides* (D1037), bombesin, human adrenocorticotropic hormone fragment 18−39 (ACTH 18−39), human angiotensin II, tris(2-carboxyethyl)phosphine (TCEP), and iodoacetamide (IAA) were obtained from Sigma-Aldrich (Taufkirchen, Germany), *N*-(3-dimethylaminopropyl)-*N*′-ethylcarbodiimid-hydrochlorid (EDC, 8.00907.0005), *N*-octyl-β-D-glucopyranoside (nOGP), trifluoroacetic acid (TFA), sodium hydrogen phosphate, ammonium carbonate from Merck (Darmstadt, Germany), streptavidin (S888) from Molecular Probes, α-cyano-4-hydroxycinnamic acid from Bruker Daltonics (Bremen, Germany), endoproteinases LysC and trypsin (sequencing grade) from Roche Diagnostics (Mannheim, Germany), somatostatin-28 from Bachem (Basel, Switzerland), disodium−hydrogenphosphate from J.T. Baker (Deventer, Netherlands), and ethylenediamine-tetraaceticacid-disodium-dihydrate (EDTA) from Roth (Karlsruhe, Germany). Acetonitrile (AcN) was purchased from Merck (HPLC gradient grade) and from Biosolve (Valkenswaard, Netherlands, super gradient grade for LC-MS). All solutions were prepared in distilled or deionized water.

Protein Expression and Purification. Targets suitable for aptamer selection were provided by the Department of Virology at the University of Cologne and Qiagen using an automated protein purification procedure for small- to large-scale high-throughput production.[42] Total RNA preparations from HIV-1 infected patients were used as templates to generate by RT-PCR cDNAs coding for HIV RT, and the V3 loop of HIV gp120.[43,44] The cDNAs were cloned into the vectors pQE-30 (Qiagen) and pGEX-2T (Amersham Biosciences, Freiburg, Germany), respectively, for bacterial expression.[45] RT comprises nucleotides 2550−4229 (p51 RT) and V3 7110−7217 (Env gp120) of HIV-1 reference strain HXB2. The vectors expressing 6×His-tagged HIV-RT (isolate 948-2) and GST-tagged HIV-gp120-V3 (isolate 138pK1) were transformed into *Escherichia coli* strains M15 [pREP4], BL21 (DE3), BL21 (DE3) Star, and BL21 (DE3) pLysS. Transformed bacteria were plated on selective LB agar, and five clones from each transformation were picked at random. To identify optimal expression conditions, the following expression screening was performed at 37 and 25 °C for each clone in 5 mL cultures in 24-deep well blocks: The clones were inoculated in LB, TB, 2× YT, and TBG-M9 media. At an $OD_{600\ nm}$ of 0.8, fusion protein production was induced by 0.01, 0.1, and 1.0 mM IPTG for 4 h, and at an $OD_{600\ nm}$ of 4.0 by 1.0 mM IPTG for 1 h. Cells were pelleted and frozen at −20 °C. Proteins were purified from those cells by high-throughput processing on a BioRobot Protein workstation (QIAGEN) as described previously.[42] The clones and expression conditions yielding highest amounts of intact and soluble proteins were 6×His-RT (M15 [pREP4] in LB, 4 h with 1.0 mM IPTG, 37 °C), and GST-V3 (BL21 [DE3] pLysS in LB, 4 h with 10 μM IPTG, 25 °C), determined by Bradford analysis and SDS-PAGE. Purification of 6×His-HIV-RT by Ni-NTA Superflow (QIAGEN, 1 mL bed volume) and of GST-gp120-V3 by Glutathione Sepharose (GE Healthcare, 5 mL bed volume) single-step chomatography was scaled up linearly and performed on an ÄkTA Explorer 100 instrument. To avoid possible interference with the automated aptamer selection process, the scale-up purification of 6×His-tagged HIV-RT was modified as follows to exclude co-purification of *E. coli* nucleic acids: Cells were lysed in buffer NPI-10^{1000} plus lysozyme (50 mM NaH_2PO_4, 1 M NaCl, 10 mM imidazole, 1 mg/mL lysozyme, 1 mM spermine, 1× Complete protease inhibitor cocktail, and EDTA-free [Roche], pH 8.0) and incubated for 30 min on ice. Soluble protein was obtained by collecting the supernatant after centrifugation (30 min, 20 000*g*,

Table 1. Aptamer Sequences[a]

aptamer	target	protein size [Da]	RNA aptamer sequences (5′-biotin-$(CH_2)_6$-p-A-p)
S66A-C6	HIV1-GST V3	32670	5′-GGG AGA GGA GGG AGA UAG AUA UCA AAC AAG AUC GCG UCU ACU GGC ACA GAA AGA GCA AUG CGG AAC UAU AGC UGA GAG UUU CGU GGA UGC CAC AGG AC-3′
S68B-C5	HIV1-GST V3	41250	2′-NH_2-pyrimidine-5′-GGG AGA GGA GGG AGA UAG AUA UCA AGA UAA AAA CGC CGG CGU AGC GCU GCA GCG CAA AAA AAC ACG ACU GCU CGC ACG AGG UGA CUC AGG CAG AGA AGG CGA GUU UCG UGG AUG CCA CAG GAC-3′
S69A-C15	HIV-RT 948-2	66100 (Monomer)	5′-GGG AGA GGA GGG AGA UAG AUA UCA AAG CAU AGA UAG GAA UGG CGG CAA GUC ACG AAC GGU ACU GGA ACG CAC AAG GAG UUU CGU GGA UGC CAC AGG AC-3′

[a] Depicted are the sequences of the Aptamers S66A-C6 (RNA), S68B-C5 (2′-NH_2-pyrimidin-RNA and S69A-C15. Biotinylated aptamers contain a biotin-$(CH_2)_6$-p-A-p moiety at the 5′ site.

4 °C) and loaded onto 1 mL Ni-NTA Superflow packed in a HR 5/5 column (GE Healthcare). The columns were washed with 5 column vol of buffer NPI-10^{1000} and 5 column vol of buffer NPI-10^{25} (50 mM NaH_2PO_4, 25 M NaCl, and 10 mM imidazole, pH 8.0) and eluted in buffer NPI-250^{25} (50 mM NaH_2PO_4, 25 M NaCl, and 250 mM imidazole, pH 8.0). Eluted protein was dialyzed against 250 vol of buffer DQ-25 (50 mM Tris-HCl, 25 mM NaCl, and 10% glycerol, pH 7.0) and passed over MonoS cation and MonoQ anion exchanger columns set in series (both 1 mL, GEH). The 6×His-HIV-RT bound to the MonoQ was separated and eluted with a 20 mL gradient of buffers DQ-25 and DQ-1000 (50 mM Tris-HCl, 1 M NaCl, and 10% glycerol, pH 7.0). HIV-RT was then dialyzed against 250 vol of RT buffer (50 mM NaH_2PO_4, 25 mM NaCl, 5 mM DTT, 0.1% (v/v) IGEPAL, and 50% (v/v) glycerol, pH 7.9) and stored at −20 °C. Glutathione affinity purification of GST-V3 and GST was performed according to the manufacturer's instructions. A total of 1.6 mg of 6×His-HIV-RT (purity 92%) and 1.0 mg of both GST-V3 (purity 97%) and GST control protein for counter selection were provided for aptamer selections.

***In Vitro* Selection of Aptamers.** Aptamer selections were carried out on an automated *in vitro* selection pathway as described elsewhere.[25] Briefly, 400 pmol RNA libraries containing a 50 nucleotide random region corresponding to approximately 10^{15} different molecules were incubated with biotinylated target protein (500 nM) in 100 μL of PBS containing 3 mM $MgCl_2$ for 30 min at 37 °C and subsequently captured on streptavidin-coated magnetic beads. RNA libraries were used for GST-V3 and HIV-RT 948-2. Additionally, GST-V3 was selected with a 2′-NH_2-pyrimidine RNA library. Unbound RNA was removed by washing the beads with PBS + 3 mM $MgCl_2$. The remaining RNA ligands were denatured and amplified by reverse transcription, PCR, and RNA transcription. A total of 200 pmol of this library was used in subsequent *in vitro* selection cycles. The libraries were cloned after 12 cycles (TA cloning kit, Invitrogen) and sequenced to identify monoclonal aptamer sequences. Designations and sequences of the oligonucleotides used are given in Table 1. All aptamer stocks were stored in ddH_2O at −20 °C.

Aptamer Biotinylation. Aptamers were biotinylated at the 5′-end during *in vitro* transcription in presence of a biotin ApG starter nucleotide (IBA GmbH, Göttingen, Germany). Approximately 200 pmol DNA template was used for a 100 μL reaction in transcription buffer containing 40 mM Tris, pH 8.0; 0.05% Triton X-100; 4% PEG8000; 25 mM $MgCl_2$; 5 mM DTT, 2.5 mM of each ATP, GTP, CTP and UTP; 1 mM Bio-ApG; and 100 U T7 RNA polymerase (Biozym). The transcription was incubated overnight at 37 °C and the RNA was purified by gel electrophoresis on a denaturing 10% PAA gel.

SAW Sensor Measurements. The system used is based on specific binding of proteins to an aptamer-modified surface. The S-sens K5 biosensor (Nanofilm) allows to record online the phase shift and the amplitude *A* at a constant frequency due to binding of molecules to the surface. On the basis of the measured phase and amplitude signal, mass and viscoelastic properties can be extracted. The sensor consisted of an ST-cut quartz sensor chip in Love geometry containing five sensor elements and a surface acoustic wave reader.[6] In each injection, one single and specifically bound layer is formed. Thin gold films are supported on processed quartz wafers. A carboxymethylated dextran layer was prepared on a self-assembled monolayer (SAM) of 11-mercaptoundecan-1-ol.[7] Surface preparation was performed in flow-through. The carboxyl groups were activated with 200 mM *N*-ethyl-*N*-(dimethyaminopropyl)-carbodiimide (EDC) and 50 mM *N*-hydroxysuccinimide (NHS) to bind 200 μg/mL streptavidin S888 (Molecular Probes), forming carboxyl amides. An excess of activated unreacted NHS-esters was deactivated by 1 M ethanolamine, pH 8.5. Biotinylated aptamers (BioTEG) were attached to the sensor chip surface in PBS buffer + 3 mM $MgCl_2$. This was accomplished through binding of the biotin residues to the immobilized streptavidin.[7] Sequences are described in Table 1. Proteins HIV V3-gp120 with a mass of 30 000 Da and HIV RT, a recombinant homodimer with a mass of 132 000 Da (monomers 66 100 Da; *in vivo* RT is a heterodimer of 117 000 Da with subunits of 66 000 and 51 000 Da)[46] were bound and dilutions were performed in protein binding buffer (PBS buffer supplemented with 3 mM $MgCl_2$ and 1 mg/mL BSA) which was also used as running buffer. Excess, nonbound protein was expelled from the flow cell with the running buffer. It was possible to fully regenerate the surface down to the coupled aptamer with an injection of 0.1 N NaOH. Mobile proteins were injected at a flow rate of 40 μL/min and an injection volume of 200 μL. The total contact time was about 300 s. Analogously to our previous approach,[6] bound masses were calculated using the sensitivity of the sensor 515 [deg cm^2 ng^{-1}] under the assumption that the value is generally applicable. Additional sensitivity values have been determined for proteins in the mass range from 1500 to 150 000 Da, showing variations of less than 5%. Concentrations were calculated with the molecular weights stated.

MALDI-ToF MS Evaluation. For evaluation by MALDI-ToF MS, methods modified from Treitz et al. were applied.[8] First, the sensor chip was removed from the biosensor. The surface-bound molecules were enzymatically digested and the peptide fragments were analyzed from the sensor chip using either (1) Peptide Mass Fingerprint (PMF) in MALDI-ToF-MS, or (2) PMF and post source decay (PSD). The result of both methods was

a list of peptide mass values, the "fingerprint", of one of the evaluated proteins. Each listed fragment was matched with high specificity to peptide entries in databases to enable the identification of the original proteins.

(1) Identification of Proteins with PMF. Proteins bound to the sensor chip surface were reduced on the chip with TCEP and alkylated with IAA in the presence of nOGP in a 50 mM aqueous sodium phosphate buffer with 1 mM EDTA at a pH of 8.0. For this purpose, 8 μL of a mixture of 25 mM TCEP in 50 mM phosphate buffer, pH 8.0, 25 mM IAA in water, acetonitrile and 50 mM phosphate buffer with 1 mM EDTA, pH 8.0 (mixed 1/1/1/2) and 2 μL 10 mM nOGP in water were applied onto the sensor chip surface. The reaction proceeded for 2 h at 37 °C in a humid atmosphere. The reaction solution was removed and washed with a few microliters of water. The protein was cleaved with Lys C/P (4 μL of 40 ng /μL Lys C in 50 mM phosphate buffer, pH 8.0, and 2 μL of 10 mM nOGP in water), which cleaves the C-terminal side of lysine (K). The resulting protein fragments were eluted with 0.1% TFA, vacuum concentrated and redissolved in 3 μL 5% AcN/0.1% TFA. One microliter of the sample was dissolved in 2 μL of HCCA (1/6 of a saturated HCCA solution in 33% AcN/0.1% TFA in 80% AcN/0.1% TFA) and prepared on a 600-μm anchor target (Bruker Daltonics, Bremen, Germany). Peptide fragments were analyzed by peptide mass fingerprint (PMF) in MALDI-ToF-MS (Reflex III, Bruker Daltonics, Bremen, Germany), giving peaks based on the ionization of the single fragments. The peaks were matched with protein fragments in a Mascot Search for significant identification of the bound protein.

(2) Identification of Peptide Fragments by PMF Followed by PSD. Proteins bound to the sensor chip surface were incubated with a solution of nOGP. Fifteen microliters of 0.05% nOGP in 50 mM ammonium carbonate buffer in 10% acetonitrile (AcN) was applied onto the sensor chip surface and the chip was dried at 37 °C. The captured protein was cleaved with 15 μL of a trypsin-solution (4 μg/mL in 0.05% nOGP) for 4 h at 37 °C in a humid atmosphere. The resulting protein fragments were eluted twice each with TFA in increasing concentrations of AcN: 15 μL of 0.1% TFA, 15 μL of 0.1% TFA in 5% AcN, 15 μL of 0.1% TFA in 33% AcN and 15 μL of 0.1% TFA in 80% AcN, vacuum concentrated and redissolved in 10 μL of 0.1% TFA. One microliter of the sample was separated with nano-HPLC (Ultimate, Dionex, Idstein, Germany). Fractions were collected directly on an anchor target with spots of 600 μm in diameter (Bruker Daltonics GmbH, Bremen, Germany). A total of 0.9 μL of matrix solution (saturated HCCA in 33% AcN/0.1% TFA diluted 1 to 10 in 80% AcN/0.1% TFA) was added simultaneously to each spot. Fraction collection and target preparation was performed with a b.a.i. Probot (Dionex, Idstein, Germany). Peptide fragments were analyzed by peptide mass fingerprint (PMF) and post source decay (PSD) in MALDI-ToF-MS (Reflex III, Bruker Daltonics, Bremen, Deutschland), giving peaks based on the ionization of the single fragment. This reduces the number of peaks per fragment to a fraction mostly to all of the correct peptides and their specified modifications. For the significant identification of the bound protein, peaks were matched with protein fragments in a database search with Mascot[47] and SearchXLinks, a program for the identification of disulfide bonds, cross-linkers, and other modifications from mass spectra of proteins.[48]

Results and Discussion

The *in vitro* selections resulted in the identification of specific aptamer sequences. Three aptamers (sequences shown in Table 1) were chosen to exemplify the further analysis. The aptamers S66A-C6 (RNA) and S68B-C5 bound HIV GST-V3 protein with an apparent K_D of 402 nM and 1.2 μM, respectively, in a filter retention experiment as described previously.[49,50] The aptamer S69A-C15 bound HIV-RT 948-2 with a K_D of 135 nM.

For the experiments using the S-sens K5 biosensor, biotinylated RNA aptamers S66A-C6 and S68B-C5 (Table 1) were immobilized on the sensor chip, and mobile GST-V3 protein was bound. The signal of the sensor depends on the properties of the contacting fluid and consists of the coupling of mass to the sensor chip surface, but also its viscosity. The recorded signal was evaluated directly without the necessity to subtract background signals arising, for example, from slight differences in the buffer content. For any interaction with a sensitive layer, the sensor signal depends directly on the distance from the sensor chip surface. Figure 1 shows the overlay plot of the signal of a single experiment. The sensor chip surface was covered with aptamer S66A-C6 or S68B-C5, respectively. Binding of V3 at concentrations from 10 to 1000 nM was monitored. For concise presentation, the change of sensor phase shift signals of one out of five sensor elements on one sensor chip are expressed in degrees [°] of selected concentrations, plotted versus time, each beginning at the start of injection of the protein.

The real-time sensor curves of the K5 biosensor (Figure 1A) display the overlay plot of the monitored phase signal of V3 binding to one of the sensor elements covered with the immobilized RNA aptamer S66A-C6 at a phase shift of 15.5 ± 0.6°. Each starts at baseline level when injected during buffer-flow. Injections of different concentrations of V3 started at $t_i = 0$ s. Protein concentration reached maximal levels within the first 10 s. During the injection period, the analyte/ligand complex reached the equilibrium value at the given concentration of the binding partners. At a flow rate of 40 μL/min, the estimated duration of an injection was $\Delta t = 560$ s. The average sensor signal for the association of V3 at 1000 nM was 3.5 ± 0.33° (Figure 1B). After injection, slow dissociation of bound V3 from the aptamer surface in running buffer was detected. To determine the association kinetics of the protein to the immobilized aptamer, data were extracted from sensor signals for all concentrations using the monomolecular growth model. For evaluation of the corresponding dissociation kinetics, the exponential decay model was assumed. The changes of the sensor phase signals were fitted, and corresponding fits were applied to the signals shown in Figure 1B. For each curve, the calculated observed rate constant (k_{obs}) in the association phase was plotted versus concentration to extract kinetic data from the resulting straight line using linear regression. The calculated values were $k_{on} = 2.1 \times 10^{-6} \pm 4 \times 10^{-7}$ nM^{-1} s^{-1} and $k_{off} = 8.7 \times 10^{-3} \pm 9 \times 10^{-4}$ s^{-1}, resulting in a $K_D = 406$ nM (Figure 1B). Titration experiments by nitrocellulose filter binding were performed to compare the K_D of the protein/RNA aptamer complex in solution with that measured on the chip surface. Unspecific binding to the membrane was corrected using a reference without protein. The fraction of complexed aptamer was determined relative to the level of initially incubated aptamer and plotted against the initial protein concentration. The fitted K_D value of the RNA aptamer for protein determined in solution was about 402 nM, which is in excellent agreement with the K_D value of 406 nM (>99%)

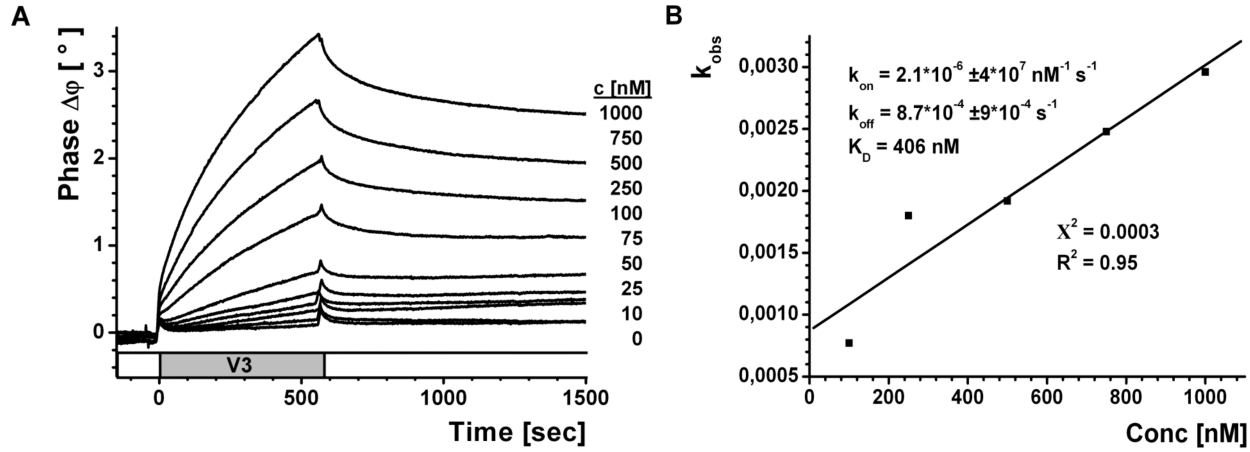

Figure 1. Binding of increasing concentrations HIV-1 V3 to aptamer S66A-C6 immobilized on the biosensor surface. (A) Prior to the measurements, biotinylated RNA aptamer S66A-C6 was coupled to a streptavidin-modified dextran layer on the sensor chip via a 5′-biotin-linker. Increasing concentrations of V3-GST were injected into a continuous buffer stream and allowed to pass the surface for 560 s (gray bar). After injection, unbound protein dissociated off in pure buffer. The surface was regenerated with 0.1 N NaOH. (B) The k_{obs} values extracted from the sensor signals in (A) plotted versus concentration of V3 protein injected. A linear best fit was applied to the data using the equation shown with k_{on} = association rate constant (on-rate) and k_{off} = dissociation rate constant (off-rate). Errors for evaluation of association usually were <5% with χ^2-test ≤0.0003 and a Fraction of Variance $R^2 > 0.95$. Linear regression had a correlation coefficient $R > 0.998$, a standard deviation of <0.001, and a probability measure of <0.0001. Errors are therefore not shown.

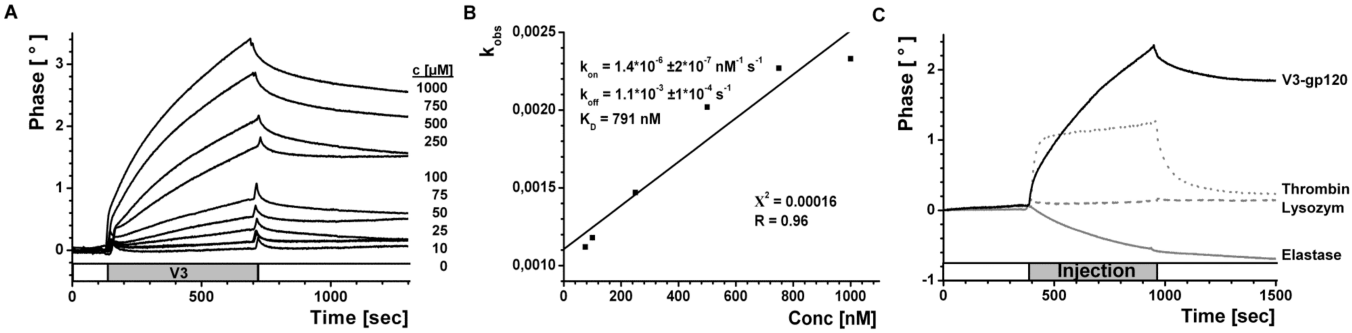

Figure 2. Binding of increasing concentrations HIV-1 V3 to aptamer S68B-C5 immobilized on the biosensor surface. (A) Prior to the measurements shown, biotinylated RNA aptamer S68B-C5 was coupled with a streptavidin-modified dextran layer on the sensor chip via a 5′-biotin-linker. Increasing concentrations of the protein were injected into a continuous buffer stream and allowed to pass the surface for a Δt as indicated by the gray bar. After injection, unbound protein dissociated off in pure buffer. The surface was regenerated with 0.1 N NaOH. (B) The k_{obs} values extracted from the sensor signals in (A) plotted versus concentration of V3 injected. A linear best fit was applied to the data using the equation shown with k_{on} = association rate constant (on-rate) and k_{off} = dissociation rate constant (off-rate). (C) Specificity of S68B-C5-modified surface. A total of 500 nM of proteins elastase, lysozyme, thrombin, and V3 was injected.

extracted from the solution/solid phase titration curves generated by the biosensor.

In a second set of binding experiments with V3, the sensor chip surface was covered with aptamer S68B-C5 (Table 1), resulting in a phase shift of 12.7 ± 0.5°. Binding of V3 was monitored (Figure 2A), and calculated k_{obs} values were plotted versus concentration of the injected fragments (Figure 2B) to extract kinetic data. The fits applied yielded a k_{on} of $1.4 \times 10^{-6} \pm 2 \times 10^{-7}$ nM^{-1} s^{-1}, a k_{off} of $1.1 \times 10^{-3} \pm 1.1 \times 10^{-4}$ s^{-1}, which results in a K_D of 791 nM. The fitted K_D value of the RNA aptamer for protein determined in solution was about 1.2 μM, which is in good agreement with the K_D value of 791 nM (64%) determined by the K5 biosensor.

We tested the S68B-C5-modified sensor chip surface for unspecific binding of proteins of the same size range. In one set of experiments, binding of 500 nM of each of the reference proteins elastase (25 900 Da), thrombin (33 600 Da) and lysozyme (14 300 Da) were measured, followed by an injection of 500 nM of the target molecule V3 (30 000 Da; Figure 2C). The phase signal increased during the injection of the reference proteins, whereas the phase shift declined rapidly after the injection was switched to pure buffer, indicating that the increase in signal is due to unspecific interactions with the sensor surface. The difference in binding after 500 s is negative for elastase (−0.7° and −39% of specific binding), and positive for thrombin 0.17° (9.5%), and for lysozyme 0.08° (4.4%). For the specifically bound V3, a phase shift of 1.8° (100%) was observed. This shows that the sensor chip surface modified with the aptamer as a ligand specifically binds the corresponding analyte V3.

Similar binding experiments were performed for HIV RT-948-2 on a surface modified with RNA aptamer S69A-C15 (Table 1), resulting in a phase shift of 11.6 ± 0.9°. Binding of RT-948-2 at concentrations from 40 to 750 nM were monitored (Figure 3A) and calculated k_{obs} values were plotted versus concentration of the injected fragments (Figure 3B) to extract kinatic data.

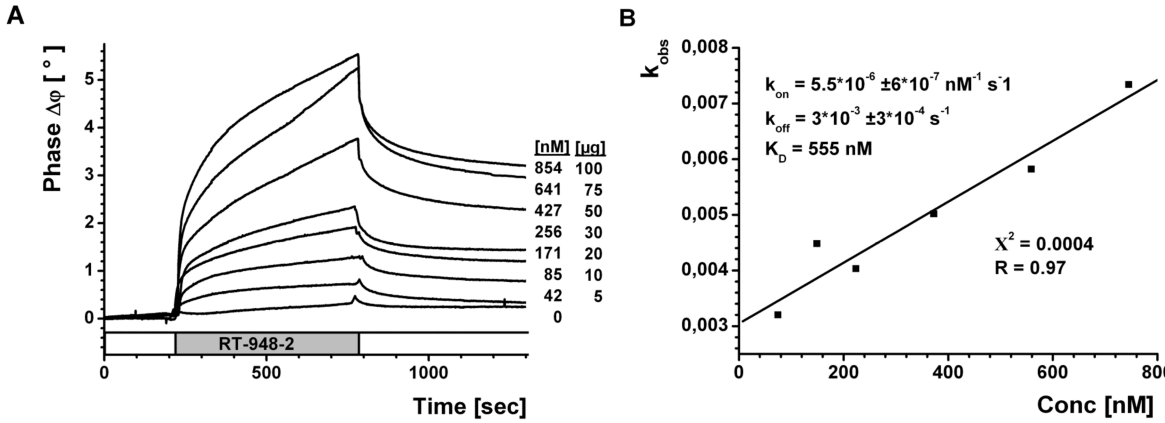

Figure 3. Binding of increasing concentrations HIV to aptamer S69 A-C15 immobilized on the biosensor surface. (A) Comparison of binding curves of HIV RT-948-2, concentrations as indicated, to biosensor chip surface regenerated with 0.1 N NaOH. Prior to the measurements shown, biotinylated RNA aptamer S69 A-C15 was coupled with a streptavidin-modified dextran layer on the sensor chip via a 5′-biotin-linker. Increasing concentrations of the protein were injected into a continuous buffer stream as described in Figures 1 and 2. The surface was regenerated with 0.1 N NaOH. (B) The k_{obs} values extracted from the sensor signals in (A) plotted versus concentration of protein injected. A linear best fit was applied to the data using the equation shown with k_{on} = association rate constant (on-rate) and k_{off} = dissociation rate constant (off-rate).

The fits applied gave a k_{on} of $5.5 \times 10^{-6} \pm 6 \times 10^{-7}$ nM^{-1} s^{-1}, a k_{off} of $3 \times 10^{-3} \pm 3 \times 10^{-4}$ s^{-1}, which leads to a K_D of 555 nM. The fitted K_D value of the RNA aptamer for protein determined in solution was 135 nM, which is in the same order of magnitude as the K_D value of 555 nM (24%) determined by the K5 biosensor.

The combination of specific protein binding with identification using MALDI-ToF MS was verified for the RNA aptamer S69 A-C15 and analyte RT-948-2. Figure 4A shows the binding of RT-948-2 (1 μM) to a sensor chip modified with S69 A-C15. The resulting phase shift of $6.3 \pm 0.24°$ equals 12.2 ng/cm^2 (i.e., 92 fmol/cm^2). For identification of the bound protein, the sensor chip was removed from the biosensor and the bound proteins were processed for on-chip identification by MALDI-ToF-MS. These steps included reduction of RT and lysis with LysC. We identified 11 fragments of sufficient intensity, from which seven fragments could be allocated (Table 2) and matched in a Mascot search (Figure 4C), resulting in sequence coverage of 10−46% (Figure 4D). With a top probability score of 89−244, and a significant ($p < 0.05$) match for CAC40518 (mass 31 626 Da), the bound protein was correctly identified as a fragment of HIV-1 RT. The corresponding complete RT has a molecular weight of about 67 100 Da, and the dimer totals to 134 200 Da.[51] The same search resulted in more than 20 further significant scores for the same protein. The observed variability among the RTs may likely be due to the increased mutation rate resulting from drug-treatment of infected humans which can lead to mutation rates of 10^{-4} (1 mutation in every 1000 base pairs).

We repeated the experiment with an alternative strategy for the identification of RT-948-2. The pure protein or the protein mixture was bound to surfaces modified with RNA aptamer S69 A-C15, resulting in matches to similar RT proteins. The proteins with the highest score for both searches were found in a publication by Quarleri et al.[52] From the mixture, NCBI entrez AAS38299 (nominal mass 56 980) was identified with a highest score of 189 at a sequence coverage of 14%. The highest match for the pure protein was NCBI entrez AAS38348 (nominal mass 57 313),[52] identified with a highest score of 244 at a sequence coverage of 10%.

Our analysis of the pair V3-GST/aptamer S68B-C5 resulted in a match of 119 residues out of 272 in total, equaling coverage of 44% (Figure 5). The fusion protein consists of the 35 amino acid long V3 loop, fused to the much larger GST, 237 amino acids in length (Figure 5). Thereby, the V3 accounts for less than 15% of the complete sequence of this protein construct. Unsurprisingly, the probability for identifying fragments resulting from the much larger GST fusion partner rather than from the V3 peptide is accordingly high. As a consequence, the queries for V3 resulted in scores considerably below the probability threshold, but only when analyzed in protein mixtures containing different concentrations of elastase, thrombin, lysozyme, and up to 10% FCS. When we analyzed the pure V3 protein, the highest score was 52 for Q1KPA8_9HIV1, a fragment of an envelope glycoprotein of HIV-1. For the 26-kDa glutathione *S*-transferase (EC 2.5.1.18) of *Schistosoma japonicum*, the highest scores were 368 when the pure fusion protein was analyzed, and 144 when the analysis was performed in the aforementioned protein mixtures. Our data show that, although the scores for the V3-GST fusion protein were below the probability threshold when analyzed in complex protein mixtures, the fusion protein could be indirectly identified with high probability scores through its fusion partner GST. A direct identification of the V3-GST fusion protein was possible when the pure protein was analyzed.

Conclusions

Mass spectrometry has proven an essential tool for the identification of proteins. Scientists have developed a number of new affinity tools to enhance the analysis of complex protein samples by adding protein separation technologies, from 1- and 2-D gel electrophoresis[53] to biosensors such as surface plasmon resonance[54] and SAW-based systems.[8] Lately, methods were developed that expand the applications, for example, to DNA chips,[55] and the coating used in established bioanalytical methods has been modified to enhance the results of the MS analysis.[56] The combination of MS with the mass-sensitive S-sens K5 technology and precleaning by binding of specific target molecules out of crude mixtures to the selective surface of an aptamer results in a considerable reduction of false-

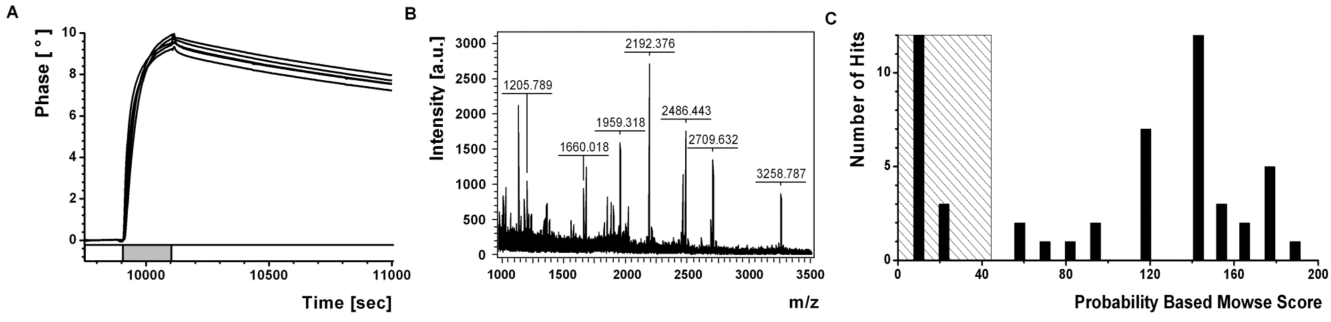


```
D   1 PQITLWQRPL VTIKIGGQLK EALLDTGADD TVLEEMNLPG RWKPKMIGGI
     51 GGFIKVRQYD QILVEICGHK AIGTVLVGPT PVNIIGRNLL TQIGCTLNFP
    101 ISPIETVPVK LKPGMDGPKV KQWPLTEEKI KALVEICTEM EKEGKISKIG
        .......... .......... .......... .......... .......KIG HIV-1 A
        .......... ........KV KQWPLTEEKI.................KIG HIV-1 B (Mix)
                                                           KIG HIV-1 C
    151 PENPYNTPVF AIKKKDSTKW RKVVDFRELN KRTQDFWEVQ LGIPHPAGXK
        PENPYNTPVF AIKK...... .KIVDFRELN KRTQDFWEVQ LGIPHPAGLK HIV-1 A
        PENPYNTPVF AIKK...... .......... .RTQDFWEVQ LGIPHPAGNK HIV-1 B (Mix)
        PENPYNTPVF AIKK...... .......... .......... .......... HIV-1 C
    201 KNKSVTVLDV GDAYFSVPLD EDFRKYTAFT IPSINNETPG IRYQYNVLPQ
        KNKSVTVLDV GDAYFSIPLD EELRKYTAFT IPSTNNETPG IRYQYNVLPQ HIV-1 A
        K......... .......... .......... .......... .RYQYNVLPQ HIV-1 B (Mix)
        K......... .......... ...RKYTAFT IPSTNNETPG IRY....... HIV-1 C
    251 GWKGSPAIFQ SSMTKILEPF RXQNPEIVIY QYVDDLYVGS DLEIGQHRTK
        GWKG...... .......... .......... .......... .......... HIV-1 A
        GWKG...... .......... .......... .......... .......... HIV-1 B (Mix)
        .......... .......... .......... .......... .........K HIV-1 C
    301 IEELRQHLLK WGFYTPDKKH QKEPPFLWXG YELHPDKWTV QPIKLPEKDS
        .......... .......... .KEPPFLWMG YELHLDKWTV QPIKL..KDS HIV-1 A
        IDELRQYLWH WGFYTPDKK. .......... .......... .......... HIV-1 C
    351 WTVNDIQKLV GKLNWASQIY PGIKVRQLCK LLRGTKALTE VVPLTAEAEL
        WTVNDIQKL. .......... .......... .......... .......... HIV-1 A
    401 ELAENREILK EPVHGVYYDP SKDLVAEIQK QGQGQWTYQI YQEPFKILKT
        .......... .......... .........K QGQGQWTYQI YQEPFKI... HIV-1 B (Mix)
    451 GKYARTRGAH TNDVKQLTEA VQKIVTESIV IWGKTPKFKL PIQKETWET
```

Figure 4. Two MALDI-ToF MS analyses of HIV RT-948-2 bound to S69A-C15 modified sensor chip surface. (A) Signals of five sensor elements at one concentration of analyte HIV RT-948-2 binding to the sensor chip surface. Prior to the measurements shown, aptamer S69A-C15 was coupled with a streptavidin-modified dextran layer on the sensor chip via a 5′-biotin-linker. Subsequently, the unbound protein was removed by the buffer flow. (B) MALDI-ToF MS spectrum of a HIV RT-948-2 digest from a chip surface. (C) Probability based Mowse top scores for protein investigated in MALDI-ToF MS. Score is $-10\times\mathrm{Log}(P)$, where P is the probability that the observed match is a random event. Protein scores greater than 64 are significant ($p < 0.05$). Only significant scores are shown. Highest scores are 89 for identified peptides displayed in Table 2A, 189 for Table 2B and 244 for Table 2C. (D) Peptides identified in (Table 2) were matched to proteins published in Online databases. Peptides were identified in Mascot Search Results, giving mass values as presented in Table 2. Shown is a match after a NCBI BLAST search to the genetically highly polymorphous HIV-1 RT AAS38299[52] with a molecular weight of 56 980. A portion of the sequence of HIV RT (fragment) is presented as a linear chain (from $-$COOH to $-NH_2$ end). Matched peptides are shown for results displayed in Table 2, resulting in sequence coverage of 46% (126 out of 273 amino acids) for Table 2A, 14% for table 2B and 10% for Table 2C. For example, for 2A, peptides with masses 1682.02, 1853.16, 1959.32, 2486.44 Da, no matches were achieved.

positive data points and an increase in the quality of the obtained data in general. Protein binding was quantified directly from the unprocessed signal, and resulted in K_D values in the same range as those determined independently by filter binding measurements. An approximate value can even be calculated from one single injection.[7] Since the isolated proteins were digested directly on the chip, the amount of the resulting analyte peptide fragments is higher than in comparable techniques. The resulting peptides contained in the unfractionated mixture were extracted and their masses identified by MALDI-ToF with high accuracy, giving a "protein ID". A database of protein sequences was queried to result in a set of likely candidate proteins. The masses were matched to protein fragment masses resulting from "virtual digestion" with the protease used in the experiment, presented in an extracted PMF peak list.

However, PMF is limited to the identification of proteins for which sequences are already known and which are stored in the database used. This poses a problem if a protein shows a high degree of variability, as is the case for many variants of HIV-1 proteins and proteins from other RNA viruses with a high mutation rate. In this study, we used proteins that originated from patients treated by the standard anti-HIV drugs currently used in the clinic, including drugs affecting the HIV-1 RT (NRTIs and NNRT). Thus, differences to the known sequences were anticipated in addition to the already high variability in HIV proteins. To overcome these limitations, fractionation by PSD was applied. The PSD data provided information on possible post-translational modifications or other variations on a protein of interest. Precursors are selected (fragmented) in series. By combination with PSD, more and precise information on a protein of interest can be gathered, which in turn improves the quality and reliability of protein identification. The GST-V3 fusion protein is an appropriate example to point out the difficulties that are encountered. Its identification in crude mixtures was focused on the GST-fraction, which is

Table 2. Mascot Search Results[a]

	start−end	observed	M_r (expt)	M_r (calc)	delta	miss	peptide sequence tag
A	50−64	1660.02	1659.01	1658.87	0.14	0	K.IGPENPYNTPVFAIK.K
	74−82	1133.77	1132.76	1132.62	0.14	0	K.IVDFRELNK.R
	83−101	2192.38	2191.37	2191.15	0.2	0	K.RTQDFWEVQLGIPHPAGLK.K
	105−126	2466.46	2465.45	2465.27	0.18	0	NK.SVTVLDVGDAYFSIPLDEELRK.Y
	127−154	3258.79	3257.78	3257.61	0.16	0	K.YTAFTIPSTNNETPGIRYQYNVLPQGWK.G
	224−245	2709.6	2708.60	2710.40	−1.7	1	K.EPPFLWMGYELHLDKWTVQPIK.L
	250−259	1205.79	1204.78	1204.57	0.21	0	K.DSWTVNDIQK.L
B	120−129	1257.68	1256.68	1256.68	0.0003	1	K.VKQWPLTEEK.I
	149−163	1659.87	1658.87	1658.87	−0.0001	0	K.IGPENPYNTPVFAIK.K
	183−200	2036.06	2035.05	2036.01	−0.9589	0	R.TQDFWEVQLGIPHPAGNK.K
	243−253	1395.75	1394.74	1394.70	0.0445	0	R.YQYNVLPQGWK.G
	431−446	2000.95	1999.94	1999.94	−0.0001	0	K.QGQGQWTYQIYQEPFK.I
C	149−163	1659.87	1658.87	1658.87	−0.0001	0	K.IGPENPYNTPVFAIK.K
	225−242	2010.03	2009.02	2009.02	−0.0001	1	R.KYTAFTIPSTNNETPGIR.Y
	226−242	1881.93	1880.93	1880.93	−0.0001	0	K.YTAFTIPSTNNETPGIR.Y
	301−318	2367.29	2366.29	2366.15	0.1373	1	K.IDELRQYLWHWGFYTPDK.K

[a] A match to CAC40518, a portion of HIV RT (fragment) is shown with a Mowse score of 89 and a total mass of 31626 Da. Seven out of 11 mass values searched were matched after a NCBI BLAST search, resulting in a sequence coverage of 126 out of 273 amino acids and a sequence coverage of 46%. No matches to peptides of masses 1682.02, 1853.16, 1959.32, 2486.44 Da were achieved. Observed, observed mass; M_r (expt), experimental m/z transformed to a relative molecular mass; M_r (calc), calculated relative molecular mass of the matched peptide; diff., difference (error) between the experimental and calculated masses; start, end of peptide sequence of the identified protein; missed, missed cleavage. (A) Peptides for protein CAC40518 identified on-chip with MALDI-ToF/peptide mass fingerprint. (B) Peptides for protein CAC40518 purified on-chip from a protein mixture and identified with MALDI-ToF/post source decay (PSD). (C)Peptides for protein CAC40518 identified on-chip with MALDI-ToF/post source decay (PSD).

```
  1-50 MSPIL GYWKI  KGLVQ PTRLL  LEYLE EKYEE  HLYER DEGDK  WRNKK FELGL
       MSPIL GYWKI  KGLVO PTRLL  LEYLE EK          DEGKD  WR  K FELGL
 51-100 EFPNL PYYID  GDVKL TQSMA  IIRYI ADKHN  MLGGC PKERA  EISML EGAVL
       EFPNL PYYID  GDVKL TQSMA  IIRYI ADK
101-150 DIRYG VSRIA  YSKDF ETLKV  DFLSK LPEML  KMFED RLCHK  TYLNG DHVTH
           DF ETLKV  DFLSK LPEML  KMFED R
151-200 PDFML YDALD  VVLYM DPMCL  DAFPK LVCFK  KRIEA IPQID  KYLKS SKYIA
                                    **** *****  *
201-250 WPLQG WQATF  GGGDH PPKSD  LVPRG SSVEI  NCTRL GNNTR  RGIHI GPGRA

251-272 FYTRE RITGD  IRQAH CNISR  TK
      E RITGD  IRQAH CNISR  TK
```

Figure 5. Match of peptides identified in MALDI-ToF MS (PMF and PSD) analysis of HIV GST-V3 bound to S68B-C5 modified sensor chip surface. Peptides identified were matched to GST-V3 which is presented as a single linear chain (from −COOH to $-NH_2$ end). The GST-part is presented in black letters. The V3 loop is presented in red letters. Matched peptides are presented in gray letters. The total number of residues is 272 from which 119 are covered, resulting in coverage of 44%.

nearly 7-times larger than the V3-portion of the fusion protein. In this case, the MALDI-ToF method itself is the limiting factor.

Taken together, our results demonstrate that highly specific aptamers were generated in the concerted approach presented. We isolated new aptamers by automated selection, which bind the HIV proteins gp120 and RT with high specificity and excellent discriminatory activity. In combination with the identification of proteins by MALDI-ToF MS, protein−protein interactions can be determined and further binding partners found.[19] Efficient binding is highly reproducible and the sensor chip surface can be regenerated to baseline levels, allowing repeated measurements on the same chip without loss of reliability. In principle, our approach should also allow to perform comparative measurements of mutant proteins from different patients.

Abbreviations: SELEX, systematic evolution of ligands by exponential enrichment; V3, third variable loop of HIV gp120; RT, reverse transcriptase; HIV-1, human immunodeficiency virus type 1.

Acknowledgment. The authors would like to thank the Ministry of Education and Research and Education (BMBF) for support (Grant No. 0312708A) of the interdisciplinary public-private partnership, the MAMS project (Microbalance Array/Mass Spectrometry). The experiments presented were performed at research center caesar, the University of Cologne, and at the QIAGEN facilities, which we would like to thank for their sustained support. We thank S. Glass, U. Schlecht and M. Perpeet for helpful discussions. We would also like to acknowledge A. Malavé and M. Schlensog for the sensor chip development and I. Stoyanov and M. Koch for the development of the fluidic system.

References

(1) Nelson, R. W.; Krone, J. R.; Jansson, O. Surface plasmon resonance biomolecular interaction analysis mass spectrometry. 1. Chip-based analysis. *Anal. Chem.* **1997**, *69* (21), 4363–4368.

(2) Nelson, R. W.; Nedelkov, D.; Tubbs, K. A. Biosensor chip mass spectrometry: a chip-based proteomics approach. *Electrophoresis* **2000**, *21* (6), 1155–1163.

(3) Mathur, S.; Badertscher, M.; Scott, M.; Zenobi, R. Critical evaluation of mass spectrometric measurement of dissociation constants: accuracy and cross-validation against surface plasmon resonance and circular dichroism for the calmodulin-melittin system. *Phys. Chem. Chem. Phys.* **2007**, *9* (47), 6187–6198.

(4) Schmidt, B.; Hoffmann, D.; Wefing, S.; Schnaible, V.; Quandt, E.; Tewes, M.; Famulok, M. *Process for Detecting Biological Molecules.* EP 01123418.4, Oct. 12, 2000.

(5) Perpeet, M.; Glass, S.; Gronewold, T.; Kiwitz, A.; Malave, A.; Stoyanov, I.; Tewes, M.; Quandt, E. SAW sensor system for marker-free molecular interaction analysis. *Anal. Lett.* **2006**, *39* (8), 1747–1757.
(6) Schlensog, M. D.; Gronewold, T. M. A.; Tewes, M.; Famulok, M.; Quandt, E. A love-wave biosensor using nucleic acids as ligands. *Sens. Actuators, B* **2004**, *101*, 308–315.
(7) Gronewold, T. M. A.; Baumgartner, A.; Quandt, E.; Famulok, M. Discrimination of single mutations in cancer-related gene fragments with a surface acoustic wave sensor. *Anal. Chem.* **2006**, *78* (14), 4865–4871.
(8) Treitz, G.; Gronewold, T. M. A.; Quandt, E.; Zabe-Kuhn, A. Combination of a SA-W-biosensor with MALDI mass spectrometric analysis. *Biosens. Bioelectron.* **2008**, *23* (10), 1496–1502.
(9) Gilligan, J. J.; Schuck, P.; Yergey, A. L. Mass spectrometry after capture and small-volume elution of analyte from a surface plasmon resonance biosensor. *Anal. Chem.* **2002**, *74* (9), 2041–2047.
(10) Gold, L.; Polisky, B.; Uhlenbeck, O.; Yarus, M. Diversity of oligonucleotide functions. *Annu. Rev. Biochem.* **1995**, *64*, 763–797.
(11) Ellington, A. D.; Conrad, R. Aptamers as potential nucleic acid pharmaceuticals. *Biotechnol. Annu. Rev.* **1995**, *1*, 185–214.
(12) Eaton, B. E. The joys of in vitro selection: chemically dressing oligonucleotides to satiate protein targets. *Curr. Opin Chem. Biol.* **1997**, *1* (1), 10–16.
(13) Wilson, D. S.; Szostak, J. W. In vitro selection of functional nucleic acids. *Annu. Rev. Biochem.* **1999**, *68*, 611–647.
(14) Famulok, M.; Hartig, J. S.; Mayer, G. Functional aptamers and aptazymes in biotechnology, diagnostics, and therapy. *Chem. Rev.* **2007**, *107* (9), 3715–3743.
(15) Srivatsan, S. G.; Famulok, M. Functional nucleic acids in high throughput screening and drug discovery. *Comb. Chem. High Throughput Screening* **2007**, *10* (8), 698–705.
(16) Famulok, M. Allosteric aptamers and aptazymes as probes for screening approaches. *Curr. Opin. Mol. Ther.* **2005**, *7*, 137–143.
(17) Famulok, M.; Mayer, G. Intramers and aptamers: applications in protein-function analyses and potential for drug screening. *ChemBioChem* **2005**, *6* (1), 19–26.
(18) Dick, L. W., Jr.; McGown, L. B. Aptamer-enhanced laser desorption/ionization for affinity mass spectrometry. *Anal. Chem.* **2004**, *76* (11), 3037–3041.
(19) Gronewold, T. M.; Glass, S.; Quandt, E.; Famulok, M. Monitoring complex formation in the blood-coagulation cascade using aptamer-coated SAW sensors. *Biosens. Bioelectron.* **2005**, *20* (10), 2044–2052.
(20) Tombelli, S.; Minunni, A.; Mascini, A. Analytical applications of aptamers. *Biosens. Bioelectron.* **2005**, *20* (12), 2424–2434.
(21) Mairal, T.; Ozalp, V. C.; Lozano Sanchez, P.; Mir, M.; Katakis, I.; O'Sullivan, C. K. Aptamers: molecular tools for analytical applications. *Anal. Bioanal. Chem.* **2008**, *390* (4), 989–1007.
(22) Hesselberth, J.; Robertson, M. P.; Jhaveri, S.; Ellington, A. D. In vitro selection of nucleic acids for diagnostic applications. *J. Biotechnol.* **2000**, *74* (1), 15–25.
(23) Ellington, A. D.; Szostak, J. W. In vitro selection of RNA molecules that bind specific ligands. *Nature* **1990**, *346*, 818–822.
(24) Tuerk, C.; Gold, L. Systematic evolution of ligands by exponential enrichment: RNA ligands to bacteriophage T4 DNA polymerase. *Science* **1990**, *249*, 505–510.
(25) Cox, J. C.; Hayhurst, A.; Hesselberth, J.; Bayer, T. S.; Georgiou, G.; Ellington, A. D. Automated selection of aptamers against protein targets translated in vitro: from gene to aptamer. *Nucleic Acids Res.* **2002**, *30* (20), e108.
(26) Blank, M.; Blind, M. Aptamers as tools for target validation. *Curr. Opin. Chem. Biol.* **2005**, *9* (4), 336–342.
(27) Weiss, S.; Famulok, M.; Edenhofer, F.; Wang, Y. H.; Jones, I. M.; Groschup, M.; Winnacker, E. L. Overexpression of active Syrian golden hamster prion protein PrPc as a glutathione S-transferase fusion in heterologous systems. *J. Virol.* **1995**, *69* (8), 4776–4783.
(28) Arendrup, M.; Akerblom, L.; Heegaard, P. M.; Nielsen, J. O.; Hansen, J. E. The HIV-1 V3 domain on field isolates: participation in generation of escape virus in vivo and accessibility to neutralizing antibodies. *Arch. Virol.* **1995**, *140* (4), 655–670.
(29) Wagner, R.; Modrow, S.; Boltz, T.; Fliessbach, H.; Niedrig, M.; von Brunn, A.; Wolf, H. Immunological reactivity of a human immunodeficiency virus type I derived peptide representing a consensus sequence of the GP120 major neutralizing region V3. *Arch. Virol.* **1992**, *127* (1−4), 139–152.
(30) Dey, A. K.; Khati, M.; Tang, M.; Wyatt, R.; Lea, S. M.; James, W. An aptamer that neutralizes R5 strains of human immunodeficiency virus type 1 blocks gp120-CCR5 interaction. *J. Virol.* **2005**, *79* (21), 13806–13810.
(31) Joshi, P.; Prasad, V. R. Potent inhibition of human immunodeficiency virus type 1 replication by template analog reverse transcriptase inhibitors derived by SELEX (systematic evolution of ligands by exponential enrichment). *J. Virol.* **2002**, *76* (13), 6545–6557.
(32) Tuerk, C.; MacDougal, S.; Gold, L. RNA pseudoknots that inhibit human immunodeficiency virus type 1 reverse transcriptase. *Proc. Natl. Acad. Sci. U.S.A.* **1992**, *89* (15), 6988–6992.
(33) Schneider, D. J.; Feigon, J.; Hostomsky, Z.; Gold, L. High-affinity ssDNA inhibitors of the reverse transcriptase of type 1 human immunodeficiency virus. *Biochemistry* **1995**, *34* (29), 9599–610.
(34) Tarrago-Litvak, L.; Andreola, M. L.; Fournier, M.; Nevinsky, G. A.; Parissi, V.; de Soultrait, V. R.; Litvak, S. Inhibitors of HIV-1 reverse transcriptase and integrase: classical and emerging therapeutical approaches. *Curr. Pharm. Des.* **2002**, *8* (8), 595–614.
(35) Andreola, M. L.; De Soultrait, V. R.; Fournier, M.; Parissi, V.; Desjobert, C.; Litvak, S. HIV-1 integrase and RNase H activities as therapeutic targets. *Expert Opin. Ther. Targets* **2002**, *6* (4), 433–446.
(36) DeStefano, J. J.; Cristofaro, J. V. Selection of primer-template sequences that bind human immunodeficiency virus reverse transcriptase with high affinity. *Nucleic Acids Res.* **2006**, *34* (1), 130–139.
(37) Hannoush, R. N.; Carriero, S.; Min, K. L.; Damha, M. J. Selective inhibition of HIV-1 reverse transcriptase (HIV-1 RT) RNase H by small RNA hairpins and dumbbells. *ChemBioChem* **2004**, *5* (4), 527–533.
(38) Hartig, J. S.; Famulok, M. Reporter ribozymes for real-time analysis of domain-specific interactions in biomolecules: HIV-1 reverse transcriptase and the primer-template complex. *Angew. Chem., Int. Ed. Engl.* **2002**, *41* (22), 4263–4266.
(39) Yamazaki, S.; Tan, L.; Mayer, G.; Hartig, J. S.; Song, J. N.; Reuter, S.; Restle, T.; Laufer, S. D.; Grohmann, D.; Krausslich, H. G.; Bajorath, J.; Famulok, M. Aptamer displacement identifies alternative small-molecule target sites that escape viral resistance. *Chem. Biol.* **2007**, *14* (7), 804–812.
(40) Hierholzer, J.; Montano, S.; Hoelscher, M.; Negrete, M.; Hierholzer, M.; Avila, M. M.; Carrillo, M. G.; Russi, J. C.; Vinoles, J.; Alava, A.; Acosta, M. E.; Gianella, A.; Andrade, R.; Sanchez, J. L.; Carrion, G.; Russell, K.; Robb, M.; Birx, D.; McCutchan, F.; Carr, J. K. Molecular Epidemiology of HIV Type 1 in Ecuador, Peru, Bolivia, Uruguay, and Argentina. *AIDS Res. Hum. Retroviruses* **2002**, *18* (18), 1339–1350.
(41) Oelrichs, R. B.; Lawson, V. A.; Coates, K. M.; Chatfield, C.; Deacon, N. J.; McPhee, D. A. Rapid full-length genomic sequencing of two cytopathically heterogeneous Australian primary HIV-1 isolates. *J. Biomed. Sci.* **2000**, *7* (2), 128–135.
(42) Schäfer, F.; Römer, U.; Emmerlich, M.; Blümer, J.; Lubenow, H.; Steinert, K. Automated high-throughput purification of 6xHis-tagged proteins. *J. Biomol. Tech.* **2002**, *13*, 131–142.
(43) Balduin, M.; Sierra, S.; Daumer, M. P.; Rockstroh, J. K.; Oette, M.; Fatkenheuer, G.; Kupfer, B.; Beerenwinkel, N.; Hoffmann, D.; Selbig, J.; Pfister, H. J.; Kaiser, R. Evolution of HIV resistance during treatment interruption in experienced patients and after restarting a new therapy. *J. Clin. Virol.* **2005**, *34* (4), 277–287.
(44) Verheyen, J.; Litau, E.; Sing, T.; Daumer, M.; Balduin, M.; Oette, M.; Fatkenheuer, G.; Rockstroh, J. K.; Schuldenzucker, U.; Hoffmann, D.; Pfister, H.; Kaiser, R. Compensatory mutations at the HIV cleavage sites p7/p1 and p1/p6-gag in therapy-naive and therapy-experienced patients. *Antivir. Ther.* **2006**, *11* (7), 879–887.
(45) Sambrook, J.; Fritsch, E. F.; Maniatis, T. *Molecular Cloning: A Laboratory Manual*; Cold Spring Harbor Laboratory Press: New York, 2001; Vol. 3.
(46) Le Grice, S. F.; Gruninger-Leitch, F. Rapid purification of homodimer and heterodimer HIV-1 reverse transcriptase by metal chelate affinity chromatography. *Eur. J. Biochem.* **1990**, *187* (2), 307–314.
(47) Hirosawa, M.; Hoshida, M.; Ishikawa, M.; Toya, T. MASCOT: multiple alignment system for protein sequences based on three-way dynamic programming. *Comput. Appl. Biosci.* **1993**, *9* (2), 161–167.
(48) Wefing, S.; Schnaible, V.; Hoffmann, D. SearchXLinks. A program for the identification of disulfide bonds in proteins from mass spectra. *Anal. Chem.* **2006**, *78* (4), 1235–1241.
(49) Famulok, M.; Hüttenhofer, A. In vitro selection analysis of neomycin binding RNAs with a mutagenized pool of variants of the 16S rRNA decoding region. *Biochemistry* **1996**, *35* (14), 4265–4270.
(50) Klug, S. J.; Hüttenhofer, A.; Famulok, M. In vitro selection of RNA aptamers that bind special elongation factor SelB, a protein with multiple RNA-binding sites, reveals one major interaction domain at the carboxyl terminus. *RNA* **1999**, *5* (9), 1180–1190.

(51) Beerenwinkel, N.; Daumer, M.; Sing, T.; Rahnenfuhrer, J.; Lengauer, T.; Selbig, J.; Hoffmann, D.; Kaiser, R. Estimating HIV evolutionary pathways and the genetic barrier to drug resistance. *J. Infect. Dis.* **2005**, *191* (11), 1953–1960.
(52) Quarleri, J. F.; Rubio, A.; Carobene, M.; Turk, G.; Vignoles, M.; Harrigan, R. P.; Montaner, J. S.; Salomon, H.; Gomez-Carrillo, M. HIV type 1 BF recombinant strains exhibit different pol gene mosaic patterns: descriptive analysis from 284 patients under treatment failure. *AIDS Res. Hum. Retroviruses* **2004**, *20* (10), 1100–1107.
(53) Henzel, W. J.; Billeci, T. M.; Stults, J. T.; Wong, S. C.; Grimley, C.; Watanabe, C. Identifying proteins from two-dimensional gels by molecular mass searching of peptide fragments in protein sequence databases. *Proc. Natl. Acad. Sci. U.S.A.* **1993**, *90* (11), 5011–5015.
(54) Krone, J. R.; Nelson, R. W.; Dogruel, D.; Williams, P.; Granzow, R. BIA/MS: interfacing biomolecular interaction analysis with mass spectrometry. *Anal. Biochem.* **1997**, *244* (1), 124–132.
(55) Tsubery, H.; Mrksich, M. Biochemical assays of immobilized oligonucleotides with mass spectrometry. *Langmuir* **2008**, *24* (10), 5433–5438.
(56) König, S. Target coatings and desorption surfaces in biomolecular MALDI-MS. *Proteomics* **2008**, *8* (4), 706–714.

PR900265R